Developmental Biology 493 (2023) 67–79

Contents lists available at ScienceDirect

Developmental Biology

journal homepage: www.elsevier.com/locate/developmentalbiology

Dorsal lip maturation and initial archenteron extension depend on Wnt11 family ligands

Elizabeth S. Van Itallie [1,*], Christine M. Field [1,**], Timothy J. Mitchison, Marc W. Kirschner

Department of Systems Biology, Harvard Medical School, Boston, MA, 02115, USA

ARTICLE INFO

Keywords:
Gastrulation
Archenteron
Blastopore
Anillin
Non-canonical Wnt
Wnt11 family

ABSTRACT

Wnt11 family proteins are ligands that activate a type of Dishevelled-mediated, non-canonical Wnt signaling pathway. Loss of function causes defects in gastrulation and/or anterior-posterior axis extension in all vertebrates. Non-mammalian vertebrate genomes encode two Wnt11 family proteins whose distinct functions have been unclear. We knocked down Wnt11b and Wnt11, separately and together, in *Xenopus laevis*. Single morphants exhibited very similar phenotypes of delayed blastopore closure, but they had different phenotypes during the tailbud period. In response to their very similar gastrulation phenotypes, we chose to characterize dual morphants. Using dark field illuminated time-lapse imaging and kymograph analysis, we identified a failure of dorsal blastopore lip maturation that correlated with slower blastopore closure and failure to internalize the endoderm at the dorsal blastopore lip. We connected these externally visible phenotypes to cellular events in the internal tissues by imaging intact fixed embryos stained for anillin and microtubules. We found that the initial extension of the archenteron is correlated with blastopore lip maturation, and archenteron extension is dramatically disrupted by decreased Wnt11 family signaling. We were aided in our interpretation of the immunofluorescence by the novel, membrane proximal location of the cleavage furrow protein anillin in the epithelium of the blastopore lip and early archenteron.

1. Introduction

Signaling mediated by Wnt11 family ligands is known to play an important role in gastrulation and anterior-posterior axis extension in all vertebrates that have been studied (Andre et al., 2015; Hardy et al., 2008; Heisenberg et al., 2000; Kilian et al., 2003; Matsui et al., 2005; Tada and Smith, 2000; Yamaguchi et al., 1999). However, the specific requirement for these ligands during gastrulation has not been fully assessed by knock-down or knock-out perturbation in amphibians. Signaling downstream of Wnt11 family ligands is complex and involves multiple membrane receptors and cytosolic proteins (Sumanas and Ekker, 2001; Wallingford, 2012). Wnt11 family ligands signal through non-canonical Wnt signaling pathways (Tada and Smith, 2000), which do not involve beta-catenin. The best characterized non-canonical pathway is the Dishevelled-dependent "Planar Cell Polarity" (PCP) pathway. In this pathway, Wnt11 family binding is thought to mediate the interaction of Dishevelled, the formin protein Daam1 (Habas et al., 2001), and RhoA, resulting in increased Rho Kinase activity which mediates changes to the cytoskeleton (Habas et al., 2001; Sato et al., 2006; Kim and Han, 2005). JNK kinase activity is also regulated downstream of Dishevelled in this pathway (Kim and Han, 2005). Even though the endogenous requirements for the Wnt11 family ligands are not known, the results of disrupting PCP signaling in explants and in whole embryos have been well characterized using the dominant interfering Dishevelled construct Xdd1 (Ewald et al., 2004; Sokol, 1996; Wallingford and Harland, 2001; Wallingford et al., 2000). This modification of Disheveled, where most of the PDZ domain is deleted, does not disrupt Adenomatous polyposis coli protein (APC) dependent degradation of beta-catenin in the canonical pathway (Wallingford et al., 2000). The model amphibian *Xenopus laevis* has played an important role in investigating the molecular biology of Dishevelled dependent PCP signaling, but the role of the Wnt11 family ligands specifically in morphogenesis of intact embryos has not been systematically investigated.

Non-mammalian vertebrate genomes typically encode two Wnt11 family proteins (Postlethwait et al., 2019). In *Xenopus laevis*, Wnt11b and Wnt11 have 63% identity at the protein level (Ku and Melton, 1993;

* Corresponding author.
** Corresponding author.
E-mail addresses: Evanitallie@gmail.com (E.S. Van Itallie), Christine_Field@hms.harvard.edu (C.M. Field).
[1] These authors contributed equally to this work.

https://doi.org/10.1016/j.ydbio.2022.10.013
Received 7 January 2022; Received in revised form 25 October 2022; Accepted 28 October 2022
Available online 2 November 2022

Garriock et al., 2005a) and are more similar to their presumed zebrafish orthologs than to each other (Supplemental Fig. 1). Xenopus Wnt11 and zebrafish Wnt11 are the homologues to the single mouse and human Wnt11 family protein, Wnt11; there is no Wnt11b in mammals (Hardy et al., 2008; Postlethwait et al., 2019). In zebrafish, morpholino knockdown of either or both Wnt11 family proteins perturbs gastrulation, with evidence for partial redundancy (Matsui et al., 2005). In *Xenopus laevis*, a Wnt11b-based dominant negative construct initially established the importance of non-canonical Wnt11 family signaling during gastrulation and for anterior-posterior axis extension (Tada and Smith, 2000). A translation blocking morpholino knockdown perturbation identified a role for Wnt11b during gastrulation when the morpholino was injected after the dorsal-ventral axis was established (Pandur et al., 2002; Tao et al., 2005). Wnt11b's mRNA expression pattern in the chordal mesoderm tissue during gastrulation is consistent with a gastrulation knock-down phenotype (Tada and Smith, 2000; Ku and Melton, 1993; Walentek et al., 2013). Wnt11 has been studied in the context of Xenopus heart development (Garriock et al., 2005a, 2005b), but whether or not it has a role during gastrulation has not been investigated.

The externally visible events of gastrulation are the formation of the blastopore, the movement of the vegetal pole and equatorial material into the blastopore, and the closure of the blastopore. The blastopore is the circular structure on the surface of the vegetal pole of the embryo that will eventually be the anus. The formation of the archenteron, which is not externally visible, is another defining event of gastrulation. Surface ectoderm cells roll over the blastopore, forming the lining of an internal cavity, the archenteron; this proto anus-to-mouth cavity becomes the gut. Complex cell and tissue-level processes including bottle cell formation, animal pole epiboly, vegetal rotation, and convergent extension are responsible for morphogenesis during gastrulation (Keller, Shook; Winklbauer, 2020). Bottle cells are epithelial cells that are extended in the apical-basal axis and have highly constricted apices. The pigment resulting from the concentration of the initially distributed pigment granules into the constricted apices is the first externally visible sign of gastrulation. Bottle cells are part of the early blastopore lip, and though they are not essential for blastopore closure, they are required for efficient closure (Keller, 1981; Hardin and Keller, 1988; Popov et al., 2018). As the archenteron extends the bottle cells are at its furthest animal, and eventually anterior, extent. Epiboly in the animal pole of embryos results in a thinning of the cell layer surrounding the blastocoel (fluid filled cavity that forms during the cleavage stages) and concomitant movement of tissue vegetally.

Vegetal rotation is responsible for the movement of the involuting mesoderm – that is on the exterior of the embryo at the beginning of the gastrulation – inside of the embryo such that it is apposed to the non-involuting mesoderm that remains closer to the surface of the embryo (Winklbauer and Schürfeld, 1999; Papan et al., 2007). Vegetal rotation, like apical constriction and convergent extension, does not occur uniformly around the embryo, but begins on the dorsal side. The force necessary for this rearrangement of the embryo largely comes from the vegetal cells, not the involuted equatorial cells, and the cellular process has been characterized and termed "ameboid-like cell migration (Wen and Winklbauer, 2017)." Convergent extension is the well-studied repacking of chordal mesoderm and neural fated cells along the medial-lateral axis that results in extension of the anterior-posterior axis relative to the dorsal-ventral and medial-lateral axes. Convergent extension is responsible for the ventral displacement of the blastopore as it closes (Keller, 1981; Pfister et al., 2016; Wilson and Keller, 1991). Convergent extension and convergent thickening drive the closure of the blastopore (Shook et al., 2018, 2022), and a later stage of vegetal rotation drives the most vegetal material animal and dorsally such that it in internalized below the closing blastopore. There are likely other cell-cell and tissue level processes that are important for the morphogenesis of these structures.

Here, we introduce anillin, a protein first known in cytokinesis and conserved from yeast to mammals (Piekny and Maddox, 2010), as a novel marker of morphogenesis in the blastopore lip and nascent archenteron. Anillin is best known as a cytokinesis furrow organizing protein which binds RhoA, F-actin, myosin II, formins, and membranes (Piekny and Maddox, 2010; Piekny and Glotzer, 2008; Straight et al., 2005; Watanabe et al., 2010; Field et al., 2005; Liu et al., 2012). In its cytokinesis role, anillin binds active RhoA and stabilizes it at the cortex, and it is necessary for stability of cleavage furrows and completion of cytokinesis (Piekny and Glotzer, 2008). It usually localizes exclusively to the nucleus in interphase cells, which is thought to provide a storage location prior to cytokinesis (Field and Alberts, 1995). However, anillin was recently shown to localize to cell junctions in interphase cells of the Xenopus animal pole epithelium, where it promotes RhoA recruitment and contractility (Reyes et al., 2014; Arnold et al., 2019). Given the connection between anillin and regulation of cortical contractility by the RhoA pathway, as well as the reports of non-cytokinesis roles of anillin in epithelium, anillin was a candidate marker for epithelial shape change during gastrulation.

We report the phenotypes from knockdown perturbations of Wnt11b and Wnt11, individually and together, in whole embryos. We identify a phenotype of failed dorsal lip maturation, failed internalization of the dorsally and animally moving vegetal material and failed initial extension of the archenteron. We also show for the first time that anillin is an excellent marker for both bottle cells and the epithelial cells that undergo morphological changes in the early blastopore and later mature blastopore lip. These studies identify both cellular and tissue-scale features affected by perturbation of Wnt11 family signaling and focus on the transition in the structure of the blastopore lip at the time period when initial extension of the archenteron is expected.

2. Methods

2.1. Normal Table illustrations

The external view vegetal pole Normal Table drawings in Supplemental Fig. 10 are from Xenbase (www.xenbase.org; RRID:SCR_003280) (Fortriede et al., 2019). Illustrations © 2021 Natalya Zahn, CC BY-NC 4.0.

2.2. Available in-situ image links

Unpublished Wnt11 in-situ images during the neurula and early tailbud stages are available at the following permanent Xenbase links:

Stage 13 – https://www.xenbase.org/entry/ViewImageActionNonAdmin.do?imageId=38631.

Stage 19 – https://www.xenbase.org/entry/ViewImageActionNonAdmin.do?imageId=38632.

Stage 21 – https://www.xenbase.org/entry/ViewImageActionNonAdmin.do?imageId=3163.

2.3. Frog use

All handling of *Xenopus laevis* adults was done in accordance with HMS IACUC protocol IS00001365. Females were injected with 500 units of human chorionic gonadotropin (HCG) to stimulate oocyte maturation and laying. All embryos result from in vitro fertilization (IVF). Embryos were cultured in 0.1x MMR at 18C unless otherwise noted (Sive et al., 2000).

2.4. Morpholinos

All morpholino injections were done at the 2-cell stage, and for all experiments morpholino was injected into both blastomeres. The morpholino amount noted for each experiment is the total amount of morpholino injected into the embryo. During injections, embryos were cultured in 0.5x MMR, 4% ficoll solution (Ficoll PM 400, Sigma). Injected embryos and fertilization matched sibling control embryos were cultured in 0.5x MMR, 4% Ficoll until they reached Stage 9 when they were

washed into 0.1x MMR. The control morpholino is the Standard Control Morpholino sold by GeneTools. The sequence of the Wnt11b morpholino (5′ to 3′) is CCAGTGACGGGTCGGAGCCATTGGT. The sequences of the Wnt11.S morpholinos (1) and (2) are CTGTATCCAAAGAGAGTTCCGAGGT and ATGAAAAGATCCTGGATTGGCAGTC, respectively (5′ to 3′). The sequence of the previously published Wnt11 morpholino is CTTCATCTTCAAAACCCAATAACAA (5′ to 3′). The five base-pair mismatch morpholino and reverse control morpholino used to assess specificity of Wnt11.S Mo2 are (5′ to 3') ATCAATAGATGCTGGATTGCCACTC and GACTGCCAATCCAGGATCTTTTCAT, respectively. Morpholinos were resuspended in water, aliquoted, and stored at −80°C. They were heated at 60°C for 10 min before combining at the appropriate concentrations for injection (Mimoto and Christian, 2011). For the Standard Control morpholino, 1 pmol equals 8.3 ng. For all of the Wnt11 family morpholinos, 1 pmol equals approximately 8.5 ng.

2.5. Still image phenotype quantification

For all quantification of end of gastrulation and tailbud stages phenotypes, the staging is done using the un-injected sibling control embryos from the same clutch. For the blastopore closure analysis from the time-lapse imaging, the frame corresponding to Stage 10.5 for all of the sibling embryos from each clutch is determined and that same frame is used as the starting point for the injected embryos from the same clutch.

2.6. Embryo holders for time lapse imaging

Custom made plastic inserts were coated with poly-hema solution and placed in the chambers of Lab-Tek II eight chambered #1.5 german cover glass systems (#155409). The chamber slide was placed in a slide holder that was attached to the microscope stage. Files for laser cutting the plastic inserts and 3D printing the slide holder can be found at: https://github.com/e-vanitallie/XLaevis_LiveImaging_Files.

2.7. Time lapse imaging

Chambers were filled with 0.75 mL of 0.1x MMR and three embryos were placed in each well. Their vegetal poles naturally oriented towards the objective lens due to gravity. The room temperature was 19°C. Time lapse images of gastrulation were collected with a Nikon Eclipse Ti2 Inverted microscope using a 4x objective lens, Zyla sCMOS camera, and Nikon Elements software. The embryos were illuminated obliquely from below using a diode light source mounted on a flexible arm. The cortical pigment granules and the color differences between cell surfaces and cell-cell interfaces provided contrast. The relatively weak oblique diode illumination did not significantly warm the embryos or perturb the embryos, so a shutter was not required. Eleven Z-plane images were acquired for each embryo every 5 min with an acquisition time between 500 and 700 ms. The Z-stacks were processed with Nikon Elements Enhanced Depth of Field (EDF). Kymographs were made with the FIJI software kymograph program (https://fiji.sc/).

2.8. Immunofluorescence

Embryos were fixed in 50 mM EGTA, ~ pH 6.8, 10% H2O, 90% methanol for at least 24 hr at room temperature with gentle shaking. After fixation the embryos were stored at 4°C. Prior to staining, embryos were rehydrated in a series of steps – 25%, 50%, 75% and 100% – methanol in TBS (50 mM Tris, pH 7.5, 150 mM NaCl for 30–45 min per step with gentle shaking. Embryos were bleached overnight in a solution of 1% H2O2, 5% formamide, 0.5x SSC (75 mM NaCl and 8 mM sodium citrate, pH 7). After bleaching, embryos were rinsed 3x in TBS and blocked in TBSN (10 mM Tris-Cl, pH 7.4, 155 mM NaCl, 1% IGEPAL CA-630, 1% BSA, 2% fetal calf serum (FCS) and 0.1% Sodium Azide) for at least an hour. Embryos were then incubated with directly labeled antibodies (diluted in TBSN) for at least 24 hr at 4°C with very gentle rotation. After antibody incubation, embryos were washed in TBSN for approximately 24 hr, with several solution changes. Embryos were dehydrated in 4 steps depending on the clearing agent used. Each dehydration step is 30–45 min. For Murray Clear (66% benzyl benzoate, 34% benzyl alcohol), wash 3x with TBS, then dehydrate in 4 steps: 30%, 50%, 70% and 100% methanol/TBS. For ethyl cinnamate (modified from (Masselink et al., 2019)), wash 3X with PBS and then dehydrate in 4 steps: 30%, 50%, 70% and 100% 1-propanol/PBS. After dehydration, embryos are transferred to a clearing solution — embryos in a small amount of methanol or 1-propanol are placed gently on top of 1.5 ml of Murray Clear or ethyl cinnamate in a 2 ml tube. As the embryos clear they fall to the bottom of the tube. The methanol or 1-propanol is removed from the top of the tube before removing the embryos for mounting. Embryos are mounted in 1.2 mm thick metal slides. The slides have a hole in the center. The hole is closed by attaching a coverslip to the bottom using heated parafilm. Another coverslip is place on top. Note: In this manuscript we have used both Murray Clear and ethyl cinnamate as clearing agents. Murray Clear and ethyl cinnamate performed identically with respect to clearing and imaging, but the latter may present less toxicity risk (Masselink et al., 2019).

2.9. Antibodies

Antibodies raised against Xenopus laevis anillin (Straight et al., 2005) and alpha-tubulin (Sigma #T6074) were labeled on a column with Alexa-568, or Alexa-647 dyes (Life Technologies, NY) as previously described (Field et al., 2017).

2.10. Microscopy immunofluorescence

Confocal Z-stack images were obtained at the Nikon Imaging Center at Harvard Medical School. Fixed Xenopus embryos were imaged using a Nikon Ti-E inverted microscope with a Nikon A1R point scanning confocal head using 10x and 20x dry objectives and NIC Elements acquisition software.

3. Results

3.1. Wnt11b and Wnt11 function in blastopore closure

We analyzed recent transcriptomic (Session et al., 2016) and proteomic (Van Itallie et al., 2021) data to confirm the presence of Wnt11b and to look for evidence of Wnt11 expression during gastrulation in *Xenopus laevis* (Supplemental Fig. 2). Wnt11b mRNA and protein are detected during this period and increase during gastrulation. Wnt11 mRNA and protein levels are much lower than those of Wnt11b, but they also increase during this period. Since both Wnt11 family proteins are present during gastrulation, we investigated the phenotypes of knock-down perturbation of the proteins individually and together.

We first used a previously published Wnt11b translation-blocking morpholino to determine the resulting phenotypes from knockdown of Wnt11b protein levels (Pandur et al., 2002; Tao et al., 2005). We injected both blastomeres at the two-cell stage because Wnt11b is expressed circumblastoporally during gastrulation (Tada and Smith, 2000; Ku and Melton, 1993). We found that Wnt11b morphant embryos exhibited more open blastopores at the end of gastrulation (Fig. 1A). Since there is no validated antibody for Wnt11b to confirm decrease in protein levels, we used a modified RNase Protection Assay to show that ribosome protected Wnt11b mRNA footprints, a proxy for translation levels, decrease with Wnt11b morpholino treatment (Supplemental Figs. 3, 4, and 5). The blastopore normally closes completely during neurulation (the morphogenic period following gastrulation where the neural folds appear and close and the anterior-posterior axis continues to extend). This also happens in the Wnt11b morphant embryos. There was no evidence of disruption of general features of the dorsal ventral asymmetry. However,

when assayed much later during the tailbud stage, most Wnt11b morphant embryos had a posterior ventral bend (Fig. 1B). The anterior-posterior axis did not appear to be shorter than in un-injected siblings. Thus, we confirmed an apparently modest role of Wnt11b in gastrulation, based on its modest morphant phenotype. (This finding is also in agreement with the recent Crispr knockout phenotype (Houston et al., 2022).)

We next considered the role of Wnt11. We confirmed the sequences of the 5′ UTRs of the transcripts of the two alloalleles for Wnt11 – Wnt11.L and Wnt11.S – and designed two different translation blocking morpholinos for each 5' UTR (Supplemental Fig. 6 for Wnt11.S morpholinos.). Injection of either Wnt11.S morpholino at either of two different doses resulted in distinctly delayed blastopore closure (Fig. 2A). Since neither Wnt11.L morpholino gave a phenotype (not shown), we continued with only the Wnt11.S morpholinos and hereafter refer to Wnt11.S as Wnt11. We also confirmed that a previously published translation blocking morpholino against Wnt11 gives the same gastrulation phenotype (Garriock et al., 2005a, 2005b), and that injection with a five base pair mismatch or a reverse sequence control morpholino does not give a reproducible gastrulation phenotype (Supplemental Fig. 7). Although available Wnt11 in-situ data does not include gastrulation stages, the well-defined Xenopus fate map, combined with evidence of expression in chordal tissues during early neurula stages, suggests that during gastrulation Wnt11 mRNA is expressed near the blastopore (Garriock et al., 2005a; Fortriede et al., 2019; Sive et al., 2000) (See **Methods** 2.2 for links). As with Wnt11b morphants, the blastopores of almost all of the embryos eventually close during neurulation and there was no evidence of disrupted dorsal-ventral axis establishment (not shown).

We also assessed the length of the anterior-posterior axis of the Wnt11 morphant embryos relative to un-injected siblings during the tailbud period (Fig. 2B). In this case, the phenotype is different from the Wnt11b morphants. For all injections of the higher dose, morphant embryos have statistically significantly shorter anterior-posterior axes. There is no bend. The shortened anterior-posterior axis phenotype is consistent with in-situ hybridization evidence of Wnt11 expression in the somites during neurulation (Garriock et al., 2005a; Fortriede et al., 2019). These data provide the first evidence for a role of Wnt11 that is similar to that of Wnt11b during gastrulation. After gastrulation, however, Wnt11's role is different from that of Wnt11b.

When we injected a 1:1 combination of the two Wnt11 morpholinos, the blastopore closure phenotype was intermediate between the two single morpholinos at 2.5 pmol and was not more severe at 5 pmol (Fig. 2A). When the phenotype was assessed at the tailbud period, the effect from the 1:1 combination increased in severity with dose (Fig. 2B). Even though we did not observe a synergistic knockdown phenotype, we interpret the similarity in phenotype of the two morpholinos as evidence that the phenotype results from on-target, additive effects. These results establish a role for Wnt11 during gastrulation in *Xenopus laevis*.

Expecting redundancy in the roles of Wnt11 and Wnt11b during gastrulation, we perturbed both proteins simultaneously. We injected embryos with a 1:1 M mixture of the Wnt11b morpholino and the Wnt11.S morpholinos (Wnt11b Mo: Wnt11 Mo1: Wnt11 Mo2 = 1:0.5:0.5). The total dose of morpholino injected was 10 pmol, compared to the maximum dose of 5 pmol used to characterize the phenotype of the Wnt11b and Wnt11 morpholinos separately. As expected, Wnt11 family morphants have larger blastopores at the end of gastrulation compared to their matched sibling embryos, whereas control morphant embryos do not (Fig. 3). In contrast to the single morphants, Wnt11 family morphants do not completely close their blastopores during neurulation (Supplemental Fig. 8). Increased total morpholino amount alone is not the cause of the stronger phenotype, as increasing morpholino amount by adding a control morpholino to 5 pmol of Wnt11 family cocktail does not result in as strong a gastrulation phenotype (Supplemental Fig. 9). These data are consistent with a partially redundant role of Wnt11b and Wnt11 during gastrulation. Therefore, we decided to pursue the double morphant approach to further characterize the role of Wnt 11 family signaling.

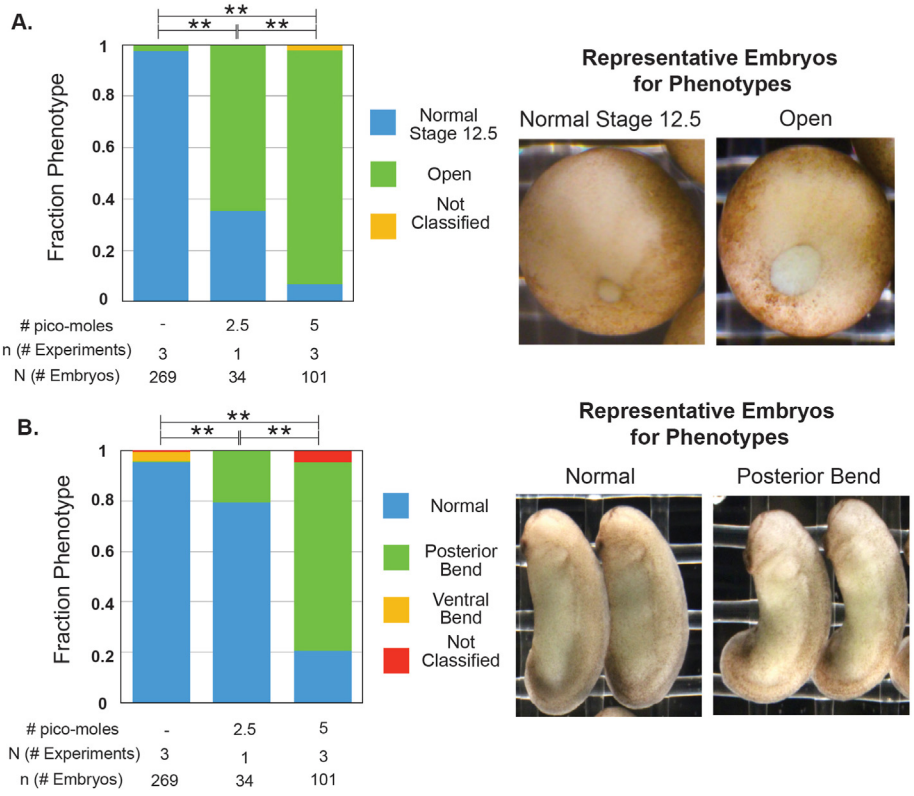

Fig. 1. Wnt11b morphant embryos have larger blastopores at the end of gastrulation and posterior bends during the tailbud period. Embryos were injected with a total of 2.5 or 5 pmol of Wnt11b Mo into both blastomeres at the 2-cell stage. **A.** Injected and sibling control embryos were classified when sibling embryos were at Stage 12.5 into two different phenotypes: normal and open blastopores. All conditions are statistically significantly different from each other (Fisher-Freeman-Halton test with BF method for multiple hypotheses; ** = p « 0.001). **B.** The same injected and sibling control embryos from **A** were classified during the tailbud period into three different phenotypes: normal, posterior bend, ventral bend (not shown). All conditions are statistically significantly different from each other (Fisher-Freeman-Halton test with BF method for multiple hypotheses; ** = p « 0.001).

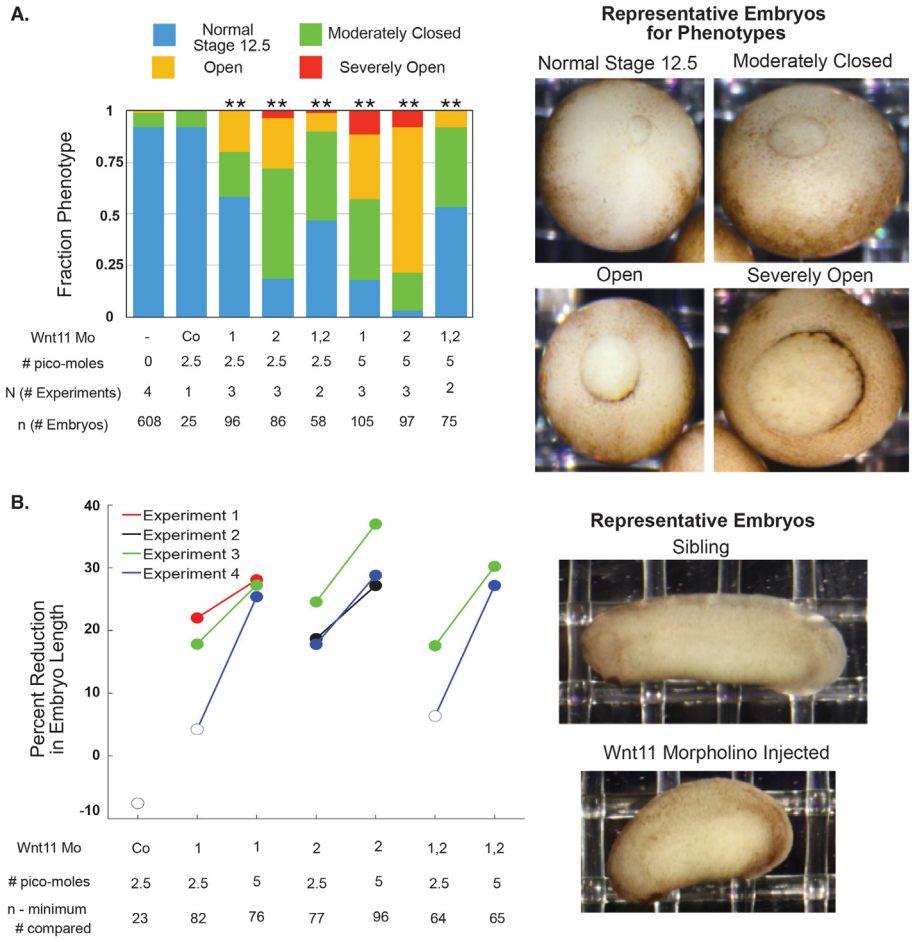

Fig. 2. Wnt11 morphant embryos have larger blastopores at the end of gastrulation and shortened anterior-posterior axes during the tailbud period. Embryos were injected with 2.5 or 5 pmol total of Wnt11 Mo1, Wnt11 Mo2, or a 1:1 mixture of both total into both blastomeres at the 2-cell stage. **A.** Injected and sibling control embryos were classified when sibling embryos were at Stage 12.5 into four different phenotypes. All injections (except the standard control morpholino) resulted in statistically significantly different proportions of the phenotypes (Chi^2 test; ** = p « 0.005). The phenotype for the 1:1 mixture of the two morpholinos is weaker than that of either of them alone. **B.** The anterior-posterior axis lengths of the embryos in **A** were quantified from still images during the tailbud period. The statistical significance of the difference in the median length between the injected and sibling embryos was tested with the Wilcoxon Rank test using the Bonferroni method to correct for multiple hypothesis testing. The percent reduction of median length is plotted with the marker filled in if the difference is statistically significant ($p < 0.05$).

3.2. Time lapse imaging reveals a Wnt11 family dependent formation of a "mature" blastopore lip

To characterize the Wnt11 family morphant phenotypes with respect to the external events of gastrulation, we performed multiplexed time-lapse imaging of the vegetal pole during gastrulation. Oblique illumination revealed cell boundaries of the blastopore lip with excellent contrast. Up to 24 embryos were imaged per experiment, allowing sibling (un-injected) embryos to be used to control for imaging conditions and timing for both control morphant and Wnt11 family morphants (Supplemental Figure 10 and **Methods** 2.6). A typical un-injected embryo is shown in Movie 1, a control morphant in Movie 2, and Wnt11 family

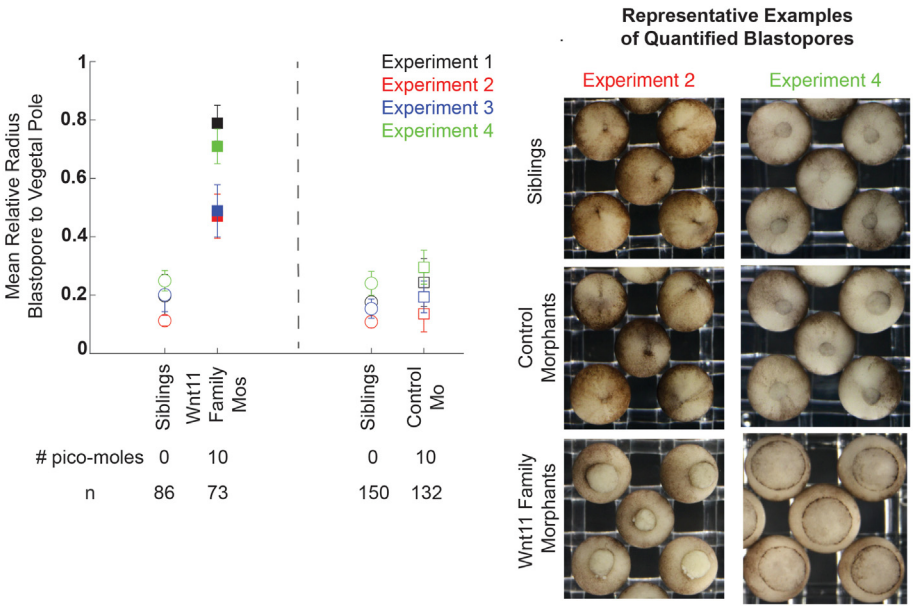

Fig. 3. Wnt11 family morphants embryos have larger blastopores at the end of gastrulation than control morphants and siblings. For four biological replicates, embryos were injected with 10 pmol total of either Wnt11 family morpholinos or the control morpholino in both blastomeres at the 2-cell stage. The relative radius of the blastopore to the embryo was quantified using FIJI processing of still images taken when siblings embryos were at Stage 12.5. The difference in relative blastopore radius was statistically significant for all replicates. The sample mean and standard deviation are shown for all biological replicates and experimental conditions. Statistical significance of the difference between the experimental injections and standard control morpholino injection values for each clutch was determined with the student's t-test, and statistically significant perturbation have filled in markers. Multiple hypothesis testing was corrected for using the Bonferroni Method. Representative example blastopores from the different conditions are shown for two biological replicates.

morphants in Movie 3 and Movie 4. Inspection of the movies showed that the Wnt11 family morphant blastopores closed more slowly, as expected from the gastrulation endpoint results. We also observe that the dorsal blastopore lip is not capable of internalizing the dorsally moving vegetal cells efficiently. There is, however, vegetal movement of the dorsal blastopore lip during the beginning of gastrulation as well as externally visible animal and dorsal movement of the vegetal cells in all of the embryos. The observation of the "overflow" of this dorsally moving vegetal material at the dorsal blastopore lip suggests defects in the morphogenesis of the blastopore lip. In Wnt11 family morphants there was transient increase of ring diameter suggesting mechanical instability of the blastopore.

Supplementary videos related to this article can be found at https://doi.org/10.1016/j.ydbio.2022.10.013

To compare and visualize dynamic features of blastopore formation and closure across the dataset, we made kymographs from the image stacks where the distance axis was a line bisecting the embryo, passing first through the dorsal lip and then across the later-forming ventral lip (Fig. 4). These kymographs capture the appearance and movement of the dorsal and ventral blastopore lips across the embryo. The closer the kymograph line is to horizontal, the faster the movement. We classified the kymographs into three phenotypes: "normal," "mildly perturbed," and "severely perturbed." In the "normal" kymographs, as time progresses, the dorsal blastopore lip line appears with a dark pigmentation and moves towards the center of the kymograph at roughly constant velocity. Later, the ventral lip pigmentation appears and also moves towards the center of the kymograph (Fig. 4A i). Then, the initially dark dorsal lip line becomes lighter in color when the bottle cells, associated with much of the pigment, have moved inside the embryo. Thus, the kymographs reveal an important transition event during gastrulation: the change of the dorsal lip from one with bottle cells on the surface to one where they have been internalized. After this internalization, we consider the dorsal blastopore lip to be a "mature lip." The mature dorsal lip line continues to smoothly move towards the ventral side of the kymographs, and the ventral line continues to move dorsally. This decreasing distance between the dorsal and ventral lip lines is the kymograph representation of the blastopore closing.

In the "severely perturbed" kymographs, which constituted 15/18 (83%) of the Wnt11 family morphant data, the dorsal and ventral lip pigmentation lines also appear and initially move towards the center of the kymograph. However, the movement of the dorsal blastopore lip is slower than in the normal kymographs, and the dark pigment color is not lost because the bottle cells with their associated pigment do not involute. Eventually, the dorsal lip line either stops moving or starts moving dorsally, i.e. the reverse of its normal ventral movement (Fig. 4A iii). When the movies corresponding to these kymographs are inspected, we see that the dorsally moving vegetal cells have overflowed the dorsal blastopore lip instead of being internalized (Movie 3 and Movie 4). Thus, the "severely perturbed" kymographs reveal the disruption of dorsal lip maturation. Without a mature lip, the embryos do not appear capable of internalizing the dorsally moving vegetal material.

We scored 2/18 (11%) of the Wnt family morphant and 4/23 (17%) of control morphant kymographs as "mildly perturbed" (Fig. 4B). In these kymographs, a small stall or reversal of the dorsal lip line occurs, but the dorsal lip eventually matures and moves ventrally (Fig. 4A ii). Based on the classification of kymographs into the three different categories, the Wnt11 family morphants are statistically significantly different than the siblings and control morphants. Eighty-three percent of the Wnt11 family

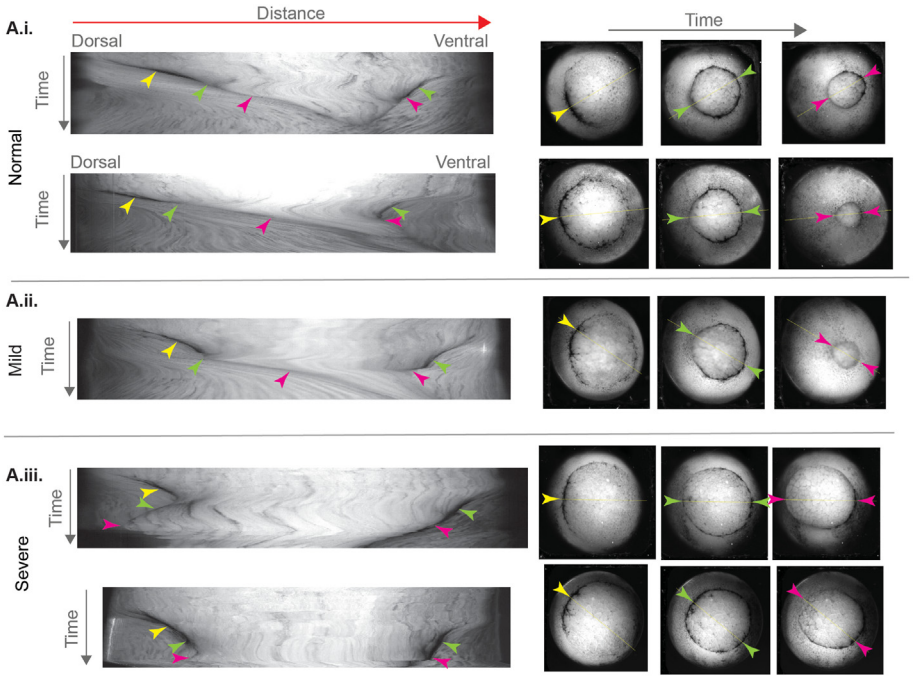

B.

	Total Number Experiments	Total Number Embryos	Normal	Mild	Severe
Siblings	6	72	69	3	0
Control Morphants	6	23	19	4	0
Wnt11 Family Morphants	5	18	1	2	15

Fig. 4. Time lapse imaging reveals blastopore lip maturation, bottle cell internalization, and blastopore closure phenotypes associated with the Wnt11 family morphants. A. Kymographs were made from the time lapse images of the vegetal pole during gastrulation. The distance axis is the line across the vegetal pole that passed first through the center of the dorsal lip and then through the center of the eventual ventral blastopore lip. The kymographs were classified into "normal," "mild perturbation," and "severe perturbation." Representative examples of the three classes are shown. In the kymographs for all three phenotypes, the dorsal bottle cells appear and move towards the center of the embryo resulting in an early lip (yellow arrowhead). In the "severe perturbation" kymographs, the movement towards the center is slower (compare **i.** and **ii.** to **iii.**). In the normal kymographs (**i.**), after the blastopore has moved further, the early lip matures and the color of the dorsal lip line changes to become lighter because the bottle cells have moved inside the embryo (dorsal green arrow). In the mild kymographs (**ii.**), this happens after transient reversal in the movement of the dorsal lip (dorsal green arrow). In the kymographs for all three phenotypes, the dark ventral lip line appears and also moves towards the center of the embryos (ventral green arrow). In the normal and mild kymographs, the dorsal and ventral lips continue to move closer to each other (pink arrowheads). By contrast, in the severe kymographs, the dorsal lip either reverses and moves away from the ventral line or stalls (dorsal pink arrowhead). **B.** Results from qualitatively scoring the kymographs from a total of five (Wnt11 family morphants) and six (sibling and control morphants) independent experiments. The Wnt11 family morphants are statistically significantly different than the control morphants and siblings (Fisher-Freeman-Halton test with BF method for multiple hypotheses; ** = $p \ll 0.001$).

morphants have the severe phenotype compared to none of the sibling or control morphants (Fig. 4B).

We also quantified the relative radius of the blastopore compared to that of the embryo for all of the time lapse movies, starting at the time point when the matched sibling embryos have just formed mature lips and internalized the bottle cells (Supplemental Fig. 11). As expected from the qualitative inspection of the movies, the Wnt11 family morphants have larger blastopore radii at this timepoint than the sibling embryos and control morphants. Then, during the time period that the siblings and control morphants completely close their blastopores, Wnt11 family morphants show only minimal blastopore closure.

The blastopore radius data and kymograph analysis together show that Wnt11 family morphants have decreased initial movement of the dorsal blastopore lip, failure to form a "mature" blastopore lip, failure to internalize the dorsally moving vegetal material, and extremely reduced blastopore closure. However, knock-down of Wnt11 family proteins does not perturb bottle cell formation or externally visible dorsal flow of the vegetal cells.

3.3. Cortical anillin marks epithelial cells in the early dorsal lip

To better understand the cell biology of Wnt11 family dependent failure of blastopore lip maturation, we sought marker proteins for visualizing the cytoskeleton during these periods. Our fixation and clearing methods made visualization of F-actin difficult. Microtubules were a good marker of cell boundaries (Lee and Harland, 2007), and we found that the cleavage furrow protein anillin provided an exceptional record of epithelial cells undergoing shape change. Both microtubules and anillin have well-established localizations during mitosis and cytokinesis, which we confirmed in dividing cells during gastrulation (Supplemental Fig. 12). These observations helped validate our fixation methods and antibodies.

Anillin exhibited dramatic enrichment at the contracting apex of bottle cells, as they initiate blastopore lip morphogenesis at Stage 10.5. Fig. 5A shows a sagittal cross-section view; see Supplemental Fig. 13 for a schematic relating this view to the exterior vegetal view of the whole embryo. Anillin was also enriched on the outside cortex of pre-bottle cells before lip invagination. Fig. 5B shows multiple horizontal cross-section views of the forming dorsal blastopore lip. In the most vegetal section, anillin is punctate and scattered along outer membranes of the cells that are changing shape. In more animal planes, anillin forms a contiguous line along the outer membranes of the cells. Since the forming blastopore lip is moving vegetally, we assume that the contiguous line is the temporally later localization. We do not know the mechanistic relevance of these two different localizations. In the horizontal cross-section view we can see that not all of the cells at the forming lip have constricted apices in this plane. Some cells are elongated, and they have the membrane proximal anillin staining. It is known that elongated cells that are not apically constricted are also part of the blastopore lip (Lee and Harland, 2007, 2010). Anillin appears to be in a membrane proximal location in cells that are changing shape. By contrast, immunofluorescence using a general membrane marker (the alpha subunit of the Na^+/K^+ ATPase) shows membrane staining in almost all cells of the embryo, in addition to moderately enhanced signal at the blastopore lip (Supplemental Fig. 14).

3.4. Wnt11 family morphants make an unsuccessful attempt to form an early dorsal lip

With anillin as a marker for the progression of lip morphogenesis, we were able to investigate the defects in Wnt11 family morphants in more detail. First, we wanted to determine how the early lip compares between siblings and Wnt11 morphants during the period before we see the phenotype of "failed lip maturation" identified in the kymograph analysis (Fig. 4). We imaged sibling, control morphant, and Wnt11 morphants fixed at the same timepoint and classified the resulting immunofluorescence images into "lip," "attempted lip," or "no lip" (Fig. 6). All of the sibling and control morphant embryos form early lips (Fig. 6D). By contrast, more than 80% of Wnt11 family morphants either have an

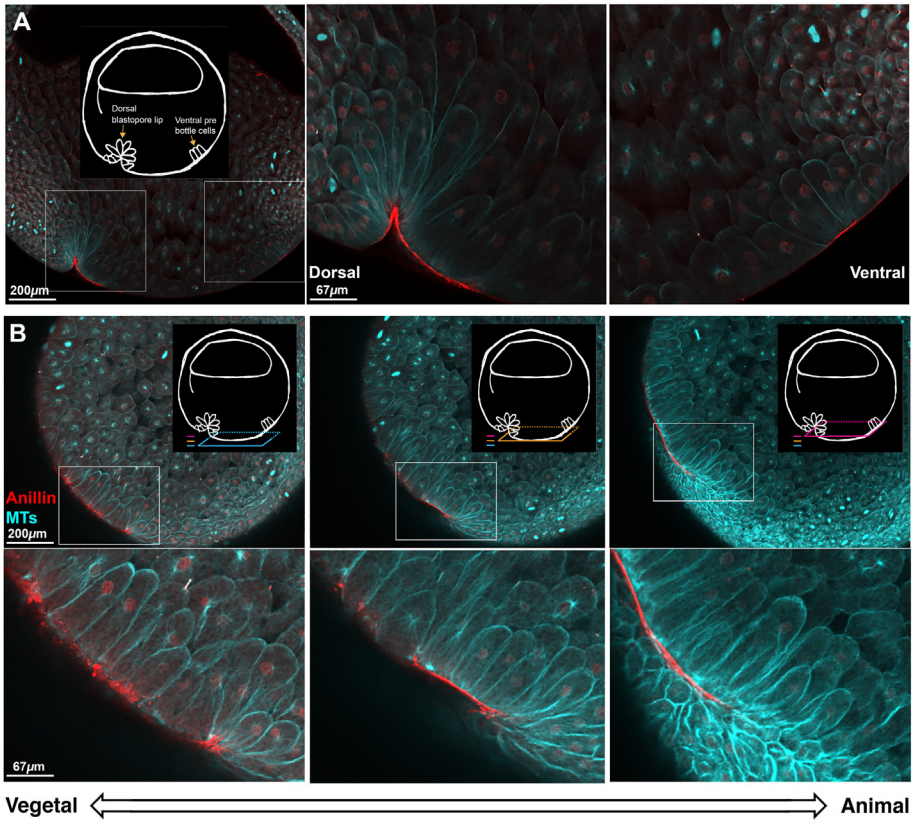

Fig. 5. Whole embryo fixed immunofluorescence against tubulin and anillin during the formation of the early dorsal blastopore lip. A. Sagittal view of a Stage 10.5 embryo shows membrane proximal anillin (red) localization to dorsal bottle cells and ventral pre-bottle cells. Tubulin (cyan) staining shows the cell outlines revealing bottle cells on the dorsal side of the embryo and elongated cells on the ventral side of the embryo. Schematic highlights the features of interest. Insets show the dorsal and ventral side of the forming blastopore lip at higher magnification. **B.** Horizontal optical plane views show distinct anillin staining patterns in different parts of the forming dorsal blastopore lip. Three colored planes show the relationship of the horizontal planes to the sagittal plane orientation in **A**, and the relationship of the horizontal planes to each other. Dorsal is left. Consistent with the sagittal view, anillin has a membrane proximal localization in elongated and apically constricted cells at the dorsal blastopore lip. In the younger, more vegetal region of the lip, the localization of anillin is punctate and in the older, more animal lip, the localization is contiguous and smooth. The z-axis span of the three planes is 90 μ m.

"attempted lip" or "no lip" at all. In all phenotypes there are cells that have membrane proximal anillin, and this anillin localization is only on the dorsal side of the embryo. This is consistent with our finding that all Wnt11 family morphants form bottle cells and that dorsal-ventral axis formation is not perturbed by the Wnt11 family knock-down. In embryos with "attempted lips," we see arcs of elongated cells that have membrane proximal anillin, but the lines of anillin are more spotted and are thinner. The attempted lip structure is also closer to the edge of the embryo. The "no lip" phenotype has puncta but no lines of anillin and also is close to the edge of the embryo.

Our immunofluorescence data of unperturbed embryos revealed that as the lip forms the anillin staining changes from spotted (Fig. 5B, left) to solid lines (Fig. 5B, center and right). The "no lip" phenotype shows the spotted localization, but there is no evidence of further progression. The "attempted lip" phenotype does have lines of anillin, but they are not as continuous or as thick as those of normal lips. The fact that more than 80% of Wnt11 family morphants have "attempted" or "no lip" lips is evidence that Wnt11 family morphant embryos can take the first early steps to make lips, but these early lips are usually not reinforced and thus the lips fail to develop properly.

3.5. Cortical anillin marks nascent archenteron extension after blastopore lip maturation

Anillin and tubulin also provided excellent markers to investigate the properties of the dorsal blastopore lip after lip maturation (Stage 11). We fixed sibling embryos during this period to determine the normal internal phenotype. Fig. 7A shows a sagittal cross-section view of anillin and tubulin staining; again, the schematic highlights features of interest. The dorsal bottle cells have moved inside the embryo and the former supra-blastoporal (above the bottle cells) and subblastoporal (below the bottle cells) endoderm now line the nascent archenteron. These cells that line the archenteron have anillin proximal to the plasma membrane (Fig. 7A, left inset, arrowhead). The staining also reveals the formation of ventral bottle cells and the ventral blastopore lip (Fig. 7A, right inset).

Fig. 7.B shows three z-planes of the horizontal view of the mature lip and upwardly extending archenteron from a representative embryo. The shapes of the cells that have anillin staining and the anillin staining itself are both different in the three panels. In the more vegetal plane, we see that the cells of the blastopore lip are columnar and show organized packing. In this optical plane, anillin has a smooth membrane proximal localization (Fig. 7B, left). As we move upward, towards the animal pole, the shape of the cells and the anillin staining change. The cells become less and less columnar, and the anillin staining becomes rougher (Fig. 7B, center). We also see that there are two lines of anillin staining with a small gap between them. This gap can also be seen in the tubulin staining, which clearly reveals cell shape. We appear to be viewing both sides of the epithelium that lines the slit-like archenteron. In the plane closest to the animal pole, the cells are the most spherical in shape and the gap between the two sides is smaller (Fig. 7B, right). When we compare the whole embryo views in the different planes, we see that the span of the anillin staining shortens as the planes move animally. This shows that during this period of gastrulation the archenteron narrows in the animal pole direction and bottle cells are at the animal extent.

3.6. Wnt11 family morphants exhibit defective archenteron extension

To investigate the role of Wnt11 family signaling in morphogenesis of the mature blastopore lip and nascent archenteron, we fixed siblings, control morphants, and Wnt11 family morphants and scored archenteron extension using anillin and tubulin staining (Fig. 8). All of the sibling and control morphant embryos show archenteron extension (Fig. 8C; see

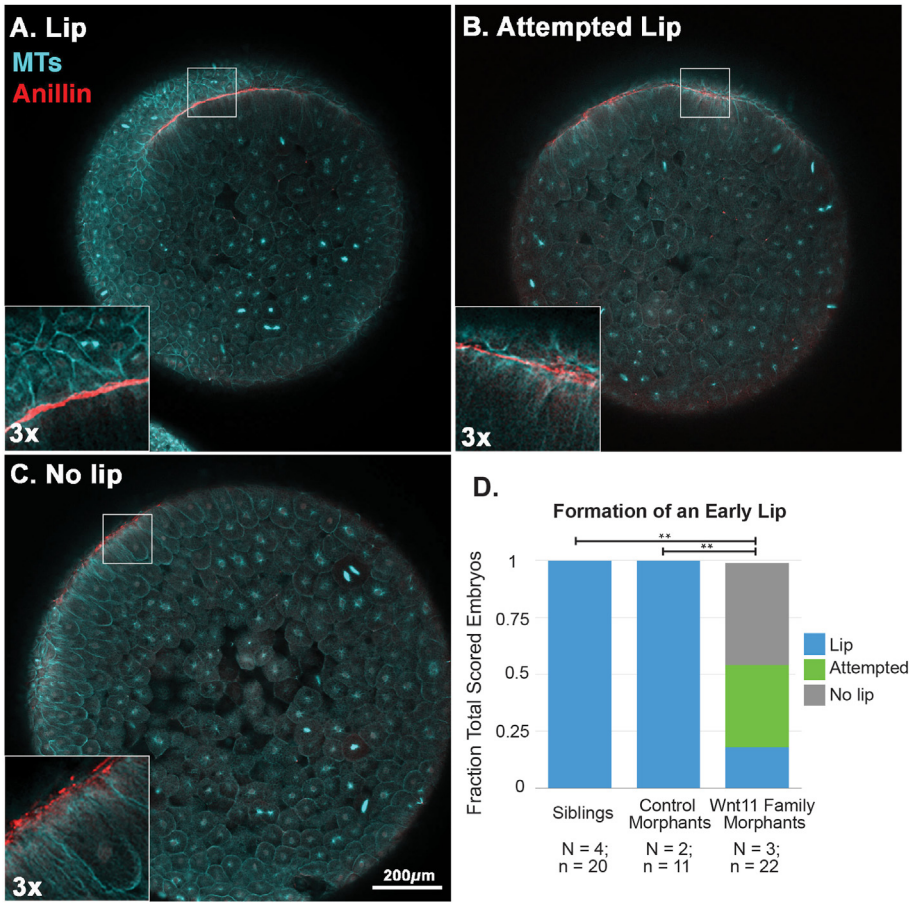

Fig. 6. Formation of an early dorsal blastopore lip is perturbed in Wnt11 family morphants. The dorsal blastopore lips of Stage 10.5 embryos were scored using anillin (red) and tubulin (cyan) immunofluorescence into **A)** Lip, **B)** Attempted Lip, and **C)** No lip phenotypes. For the "attempted lip" phenotype, we see lines of anillin, but they are not as strong or contiguous as in the "lip" phenotype. The "no lip" phenotype only has spots of anillin. The results are summarized in **D.** Wnt11 family morphants are statistically significantly different from the sibling and control morphant embryos (** = p« 0.05).

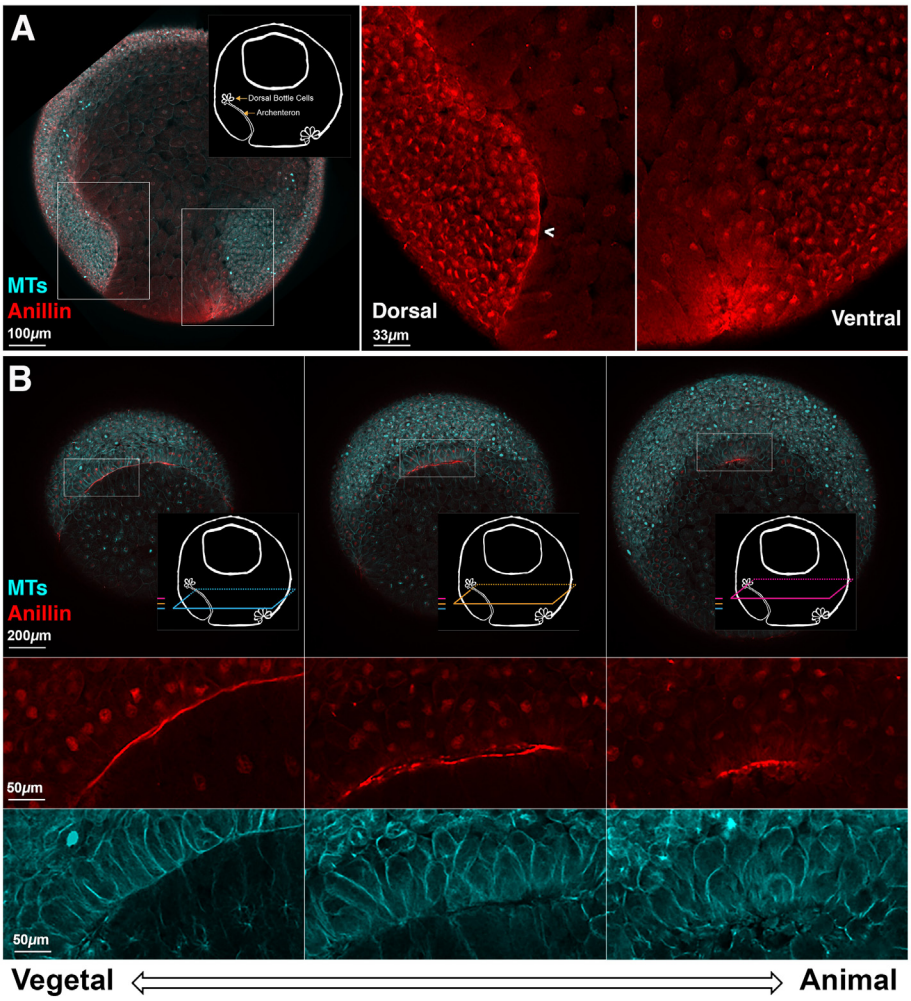

Fig. 7. Whole embryo fixed immunofluorescence against tubulin and anillin after dorsal lip maturation enables visualization of the extending archenteron. A. Sagittal view of a Stage 11 embryos shows membrane proximal anillin (red) staining along the mature dorsal and immature ventral blastopore lips. There is anillin staining along the animally extending archenteron. Schematics highlight the features of interest. Insets show the dorsal and ventral sides of the blastopore with higher magnification. **B.** Horizontal optical plane views show the differences in anillin staining and cell shape in different regions of the mature lip and archenteron. As in Fig. 6, the three colored planes show the relationship of the horizontal optical planes to the sagittal plane image in **A** and the relationship of the horizontal planes to each other. Dorsal is up. At the mature dorsal lip (most vegetal), the anillin staining is often in regions of packed columnar or square cells. In these regions, the anillin appears as a line apically. As the planes move animally, the anillin staining is more spotted, and the cells are various shapes that are neither square nor spherical. When the planes are compared, the span of the anillin arc gets shorter as the planes progress upward from vegetal to animal. The anillin is marking the upwardly extending archenteron. The z-axis span of the three planes is 75 μ m.

Fig. 8A for representative example very similar to Fig. 7). However, ~90% of Wnt11 family morphants show no evidence of archenteron extension (see Fig. 8B for two representative examples). In these embryos, we do not see the overlaying arcs of anillin as the planes move animally, nor do we see any evidence of a short arc of bottle cells at the animal extent of the planes of membrane proximal anillin staining. In one of the "no extension" examples (Fig. 8B top panels), we do see a successfully formed early lip. This is the only example in our data where we see a successful early lip in a morphant at this timepoint. The other example (Fig. 8B bottom panels) has multiple foci of membrane proximal anillin in most vegetal plane, but they have not progressed to a correctly formed early lip. Supplemental Fig. 15 shows a matched sibling and Wnt11 family morphant embryo set from the time point that developed furthest prior to fixation. In the siblings, the bottle cells at the anterior extent of the archenteron have started to spread; however, there is still no evidence of a mature dorsal lip in the Wnt11 morphants or evidence of archenteron extension.

4. Discussion

Amphibian embryos have always played a large role in understanding the morphogenesis that takes place between the spherical egg, a geometry shared by many organisms, and the vertebrate body plan (Holtfreter, 1944). The initial starting conditions of egg shape and yolk distribution, which vary greatly across vertebrates, are important to the strategies of gastrulation (Gerhart and Kirschner, 1997), but there is evidence that some of the cell and tissue level behaviors, as well as the signaling pathways that control them, are conserved (Chuai et al., 2021; Serra et al., 2021). One of these widely used signaling pathways is Dishevelled dependent non-canonical Wnt signaling. We have learned a great deal about the molecular players involved in non-canonical Wnt signaling, but we still have an imperfect idea of how a process like gastrulation uses these pathways at the tissue level.

Our study began with an attempt to understand the roles of the two Wnt11 family proteins Wnt11 and Wnt11b, thought to be agonists in the non-canonical Wnt pathway. This is the first experimental paper, to our knowledge, that has explicitly addressed the function of the two Wnt11 family members in *Xenopus laevis* during gastrulation. In what we report here, this investigation leads to very fundamental questions, such as how the blastopore forms, how the vegetal endoderm is internalized, and how the archenteron initially extends. We have expanded upon the existing methods of imaging embryos. Our set-up for multiplexed oblique illumination microscopy allows for direct comparison of embryos across eight different conditions, and the open source instructions for this set-up will be useful for other labs. The resulting movies of the vegetal pole and our kymograph analysis led to the finding that Wnt11 family proteins signal to promote blastopore lip maturation, internalization of the vegetal material, and blastopore closure. Disruption of all of these Wnt11 family dependent processes has been reported in *Xenopus laevis* embryos perturbed with dominant negative Dishevelled, which provides strong evidence that the Wnt11 family signaling during gastrulation is Dishevelled dependent (Ewald et al., 2004). Immunofluorescence has been used previously, but here we have added new markers, in whole embryos, which provide new views of these classic morphogenetic processes. We

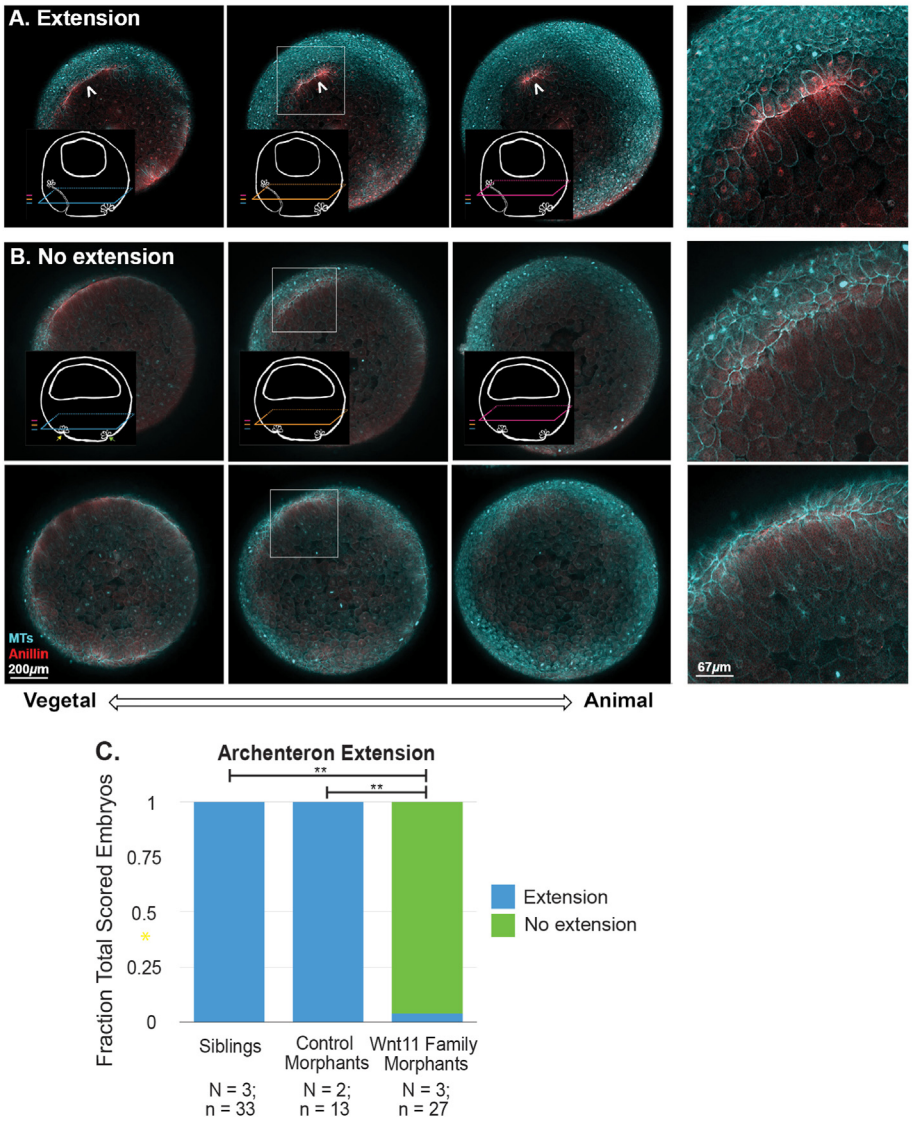

Fig. 8. Archenteron extension in perturbed in Wnt11 family morphants. Archenteron extension in Stage 11 embryos was scored using anillin (red) and tubulin (cyan) immunofluorescence. The embryos were classified into **A)** Extension and **B)** No extension phenotypes (two different examples). By contrast to the "extension" phenotype, the "no extension" embryos do not have arcs of membrane proximal anillin staining in the more animal planes; only cytoplasmic anillin signal is seen in the zoom insets. The top "no extension" example shows evidence of a late forming "early lip." However, no archenteron extension is seen. The lower example is more representative of what is seem in the Wnt11 family morphants. The z-axis span of the three planes is 85 μ m. The results of scoring sibling, control morphant, and Wnt11 family morphants are summarized in **C.** Wnt11 family morphants are statistically significantly different from the sibling and control morphant embryos (** = p« 0.05).

report strong enrichment of anillin in the outer cortex of epithelial cells in the blastopore lip and archenteron, which allowed us to use anillin as a cytological marker for epithelial dynamics in the gastrula. Furthermore, Supplemental Fig. 16 shows that membrane proximal localization of anillin in the archenteron epithelium and at the blastopore continues through Stage 12.5, indicating that anillin could be used as a marker for studying archenteron morphogenesis after its initial extension as well (Keller, Shook; Nieuwkoop and Faber, 1994).

Our observation of the overflowing vegetal material at the dorsal blastopore lip raises questions about the relationship between vegetal rotation and the processes including bottle cell formation, convergent extension, and convergent thickening that are necessary for normal closure of the blastopore. During the first half of gastrulation in normally developing embryos, the dorsal lip moves vegetally due to vegetal rotation and epiboly, and the marginal mesendoderm involutes (Fig. 9A). We observe some movement of the dorsal blastopore lip during the first half of gastrulation, but not as much as in siblings and control morphants (see Fig. 4 and Supplemental Fig. 11). One of the most important processes that takes place during the period is the involution of the marginal zone mesendoderm driven by vegetal rotation and epiboly. In this paper, we have not explicitly addressed involution of the marginal zone mesendoderm; however, Ewald et al. found that in embryos perturbed with dominant negative Dishevelled, the marginal mesendoderm does involute (Ewald et al., 2004).

During the second half of gastrulation in normally developing embryos, the non-involuted and involuted chordal tissue begin the mediolateral intercalation behavior of convergent extension and the dorsal lip continues to move vegetally (Fig. 9B). The large vegetal cells continue to move dorsally and animally and pass under the dorsal lip. In our Wnt11 family morphants, this is the period when we observe our strongest phenotypes: failure of bottle cells to leave the dorsal blastopore lip and an inability of the dorsal blastopore lip to contain the animally and dorsally moving vegetal tissue (Fig. 9C). This work does not investigate which morphogenic process are perturbed during this period. Defects in vegetal rotation during this period may be partially responsible for this phenotype. We do, however, observe some dorsal, animal movement of the vegetal material, and thus we suspect that vegetal rotation is occurring to some degree. Defects in convergent extension could also contribute to the observed phenotype at the dorsal lip. In the Wnt11 morphants, the dorsal lip shows limited vegetal movement immediately following the failure of lip maturation. Many previous studies have identified Dishevelled dependent non-canonical Wnt signaling to be crucial for convergent extension (Ewald et al., 2004; Wallingford et al., 2000). Defects in both vegetal rotation and convergent extension would be expected to affect the location of bottle cells during gastrulation. Bottle cells should move animally in the same direction as the vegetal material following lip

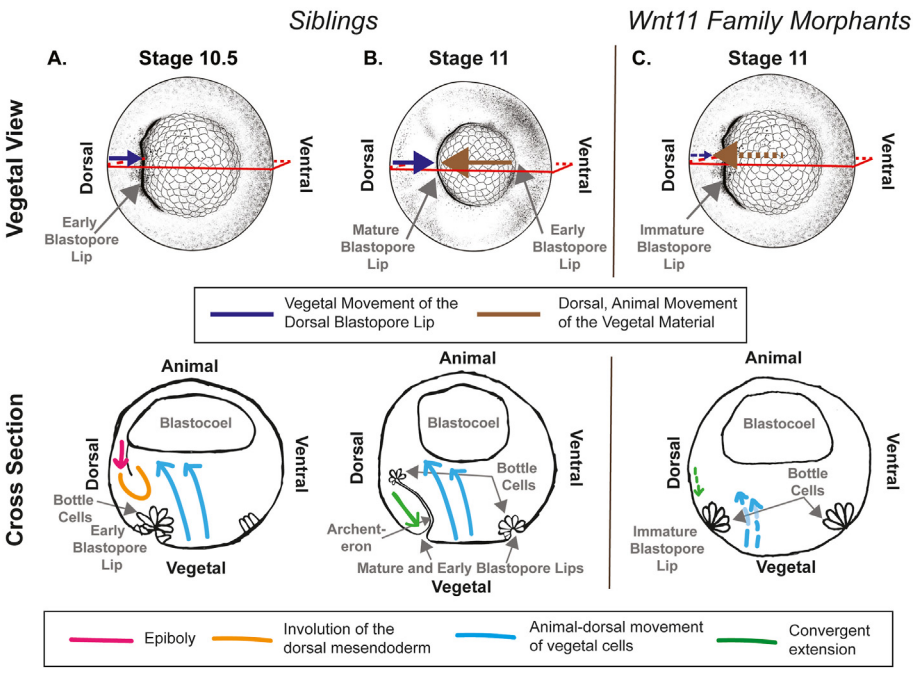

Fig. 9. Comparison of external and internal phenotypes observed in sibling and Wnt11 family morphants. Top panel shows the vegetal view of the embryos with the externally visible phenotype, and the bottom panel shows cartoons of a cross sectional view with internal events indicated. **A.** During Stage 10.5, we observe the dorsal blastopore lip moving vegetally (upper panel, purple). This is due to epiboly (bottom panel, pink) and vegetal rotation (bottom panel, blue) that move the marginal zone mesendoderm deeper in the embryo (bottom panel, orange). **B.** During Stage 11, we observe the dorsal blastopore lip continuing to move vegetally (upper panel, purple), and the vegetal material moves animally and dorsally under the dorsal blastopore lip. The blastopore lip movement is now largely due to convergent extension (bottom panel, green). Continuing vegetal rotation movements (upper panel, blue) drive the vegetal material under the dorsal blastopore lip. The archenteron has extended and bottle cells remain at the animal extent. **C.** In the Wnt11 family morphants, we observe moderate vegetal movement of the dorsal blastopore lip (upper panel, small purple arrow) before and during Stage 10.5, and very little after Stage 11. The vegetal material does move animally and dorsally (upper panel, brown arrow) and overflows the dorsal blastopore lip. We also observed that the archenteron does not extend, and the bottle cells remain at the surface of the embryo. The dashed lines indicate processes that are likely affected by knockdown of the Wnt11 family ligands (convergent extension - green, vegetal rotation - blue).

maturation, but in the Wnt11 family morphants this does not happen, and they remain visible on the embryo surface until the overflowing vegetal material occludes them from view.

Successful maturation of the blastopore lip requires not only that multiple morphogenic processes take place simultaneously, but that they co-occur in such a way that necessary physical properties such as tension and deformability are achieved. We have shown for the first time that the actin and myosin binding and membrane organizing protein anillin has a specific membrane proximal localization in the blastopore and dorsal blastopore lip during gastrulation. We found that both the tissue organization of the epithelial cells of the dorsal blastopore lip and the anillin staining was very different in the sibling and Wnt11 family morphants. These differences between sibling and Wnt11 family morphants, in addition to anillin's known role in organizing membrane related structures (Piekny and Maddox, 2010), suggests that anillin's possible role in maintaining tension and structural integrity of the lip is dependent on Wnt11 family signaling. Actin and myosin-II have been implicated in gastrulation morphogenesis in many studies (Popov et al., 2018; Pfister et al., 2016; Lee and Harland, 2007), but there has been little analysis of more specialized cortical proteins and their regulation. Our finding that anillin, and possibly also ERM (ezrin, radixin, moesin) family proteins (Sato et al., 1991, 1992) (Supplemental Fig. 17), selectively localize to the cortex of certain cells during gastrulation provides a starting point for future studies that may inform our understanding of the connection between signaling pathways and physical requirements for correct tissue organization during gastrulation. Answering these questions will require studies in whole embryos where the effects of signaling on the mechanics of events occurring in multiple tissues can be assessed simultaneously.

Author contributions

Elizabeth Van Itallie: Conceptualization, Investigation, Writing – Original Draft, Writing – Review & Editing; Christine M. Field: Conceptualization, Investigation, Writing – Review & Editing; Timothy J. Mitchison: Resources, Writing – Review & Editing, Funding Acquisition. Marc W. Kirschner: Writing – Review & Editing, Funding Acquisition.

Data availability

Data will be made available on request.

Acknowledgements

Funding to TJM from GM131753 and to MWK from HD073104. The authors acknowledge the Nikon Imaging Center at Harvard Medical School for microscopy and image analysis resources. Stirling L. Churchman and Blake Tye (Harvard Medical School, Department of Genetics) helped with confirmation of polysome stabilization. Additionally, Leonid Peshkin and Jenny Gallop first conceived of the embryo holders used for the inverted external imaging, and Rachael Jonas-Closs provided exceptional Xenopus husbandry.

Appendix A. Supplementary data

Supplementary data to this article can be found online at https://doi.org/10.1016/j.ydbio.2022.10.013.

References

Andre, P., Song, H., Kim, W., Kispert, A., Yang, Y., 2015. Wnt5a and Wnt11 regulate mammalian anterior-posterior axis elongation. Development 142 (8), 1516–1527, 25813538.

Arnold, T.R., Shawky, J.H., Stephenson, R.E., Dinshaw, K.M., Higashi, T., Huq, F., Davidson, L.A., Miller, A.L., 2019. Anillin regulates epithelial cell mechanics by structuring the medial-apical actomyosin network. Elife 8, e39065, 30702429.

Chuai, M., Nájera, G.S., Serra, M., Mahadaven, L., Weijer, C.J.. Reconstruction of distinct vertebrate gastrulation modes via modulation of key cell behaviours in the chick embryo [Internet]. [cited 2021 Dec 30]. Available from: https://www.biorxiv.org/content/10.1101/2021.10.03.462938v3.

Ewald, A.J., Peyrot, S.M., Tyszka, J.M., Fraser, S.E., Wallingford, J.B., 2004. Regional requirements for Dishevelled signaling during Xenopus gastrulation: separable effects on blastopore closure, mesendoderm internalization and archenteron formation. Development 131 (24), 6195–6209.

Field, C.M., Alberts, B.M., 1995. Anillin, a contractile ring protein that cycles from the nucleus to the cell cortex. J. Cell Biol. 131 (1), 165–178, 7559773.
Field, C.M., Coughlin, M., Doberstein, S., Marty, T., Sullivan, W., 2005. Characterization of *anillin* mutants reveals essential roles in septin localization and plasma membrane integrity. Development 132 (12), 2849–2860, 15930114.
Field CM, Pelletier JF, Mitchison TJ. Xenopus extract approaches to studying microtubule organization and signaling in cytokinesis. In: Methods in Cell Biology [Internet]. Elsevier; 2017 [cited 2021 May 25]. p. 395-435. Available from: https://linkinghub.elsevier.com/retrieve/pii/S0091679X16300486.
Fortriede, J.D., Pells, T.J., Chu, S., Chaturvedi, P., Wang, D., Fisher, M.E., James-Zorn, C., Wang, Y., Nenni, M.J., Burns, K.A., Lotay, V.S., Ponferrada, V.G., Karimi, K., Zorn, A.M., Vize, P.D., 2019. Xenbase: deep integration of GEO & SRA RNA-seq and ChIP-seq data in a model organism database. Nucleic Acids Res. 31733057.
Garriock, R.J., D'Agostino, S.L., Pilcher, K.C., Krieg, P.A., 2005a. Wnt11-R, a protein closely related to mammalian Wnt11, is required for heart morphogenesis in Xenopus. Mar Dev. Biol. 279 (1), 179–192.
Garriock, R.J., D'Agostino, S.L., Pilcher, K.C., Krieg, P.A., 2005b. Corrigendum to "Wnt11-R, a protein closely related to mammalian Wnt11, is required for heart morphogenesis in Xenopus" [Dev. Biol. 279. Dev. Biol. 179–192, 2008 Oct;322(1): 235.
Gerhart, J.C., Kirschner, M.W., 1997. Cells, Embryos and Evolution. Wiley.
Habas, R., Kato, Y., He, X., 2001. Wnt/Frizzled activation of Rho regulates vertebrate gastrulation and requires a novel formin homology protein Daam1. Cell 107 (7), 843–854, 11779461.
Hardin, J., Keller, R., 1988. The behaviour and function of bottle cells during gastrulation. Development 103 (1), 211–230, 3197630.
Hardy, K.M., Garriock, R.J., Yatskievych, T.A., D'Agostino, S.L., Antin, P.B., Krieg, P.A., 2008. Non-canonical Wnt signaling through Wnt5a/b and a novel Wnt11 gene, Wnt11b, regulates cell migration through avian gastrulation. Dev. Biol. 320, 391–401, 18602094.
Heisenberg, C.P., Tada, M., de, L.S., Concha, M.L., Geisler, R., Stemple, D.L., Smith, J.C., Wilson, S.W., 2000. Silberblick/Wnt11 mediates convergent extension movements during zebra®sh gastrulation, 405, p. 6.
Holtfreter, J., 1944. A study of the mechanics of gastrulation. J. Exp. Zool. 95 (2), 171–212.
Houston, D.W., Elliott, K.L., Coppenrath, K., Wlizla, M., Horb, M.E., 2022. Maternal Wnt11b regulates cortical rotation during *Xenopus* axis formation: analysis of maternal-effect *wnt11b* mutants. Development 149 (17), dev200552, 35946588.
Keller, R.E., 1981. An experimental analysis of the role of bottle cells and the deep marginal zone in gastrulation of Xenopus laevis. J. Exp. Zool. 216, 81–101.
Keller R, Shook D. Gastrulation in Amphibians. In: Gastrulation: from Cells to Embryo. p. 171–203.
Kilian, B., Mansukoski, H., Barbosa, F.C., Ulrich, F., Tada, M., Heisenberg, C.P., 2003. The role of Ppt/Wnt5 in regulating cell shape and movement during zebrafish gastrulation. Apr Mech. Dev. 120 (4), 467–476.
Kim, G.H., Han, J.K., 2005. JNK and ROK? function in the noncanonical Wnt/RhoA signaling pathway to regulateXenopus convergent extension movements. Apr Dev. Dynam. 232 (4), 958–968.
Ku, M., Melton, D.A., 1993. Xwnt-11: a maternally expressed Xenopus wnt gene. Development 119, 1161–1173.
Lee, J.Y., Harland, R.M., 2007. Actomyosin contractility and microtubules drive apical constriction in Xenopus bottle cells. Dev. Biol. 13, 17868669.
Lee, J.Y., Harland, R.M., 2010. Endocytosis is required for efficient apical constriction during Xenopus gastrulation. Curr. Biol. 20 (3), 253–258, 20096583.
Liu, J., Fairn, G.D., Ceccarelli, D.F., Sicheri, F., Wilde, A., 2012. Cleavage furrow organization requires PIP2-mediated recruitment of anillin. Curr. Biol. 22 (1), 64–69, 22197245.
Masselink, W., Reumann, D., Murawala, P., Pasierbek, P., Taniguchi, Y., Bonnay, F., Meixner, K., Knoblich, J.A., Tanaka, E.M., 2019. Broad applicability of a streamlined Ethyl Cinnamate-based clearing procedure. Development, 166884 dev. 30665888.
Matsui, T., Raya, A., Kawakami, Y., Callol-Massot, C., Capdevila, J., Rodriguez-Esteban, C., Belmonte, J.C.I., 2005. Noncanonical Wnt signaling regulates midline convergence of organ primordia during zebrafish development. Genes Dev. 19, 164–175, 15630025.
Mimoto, M.S., Christian, J.L., 2011. Manipulation of Gene Function in Xenopus laevis [cited 2021 Apr 19]. In: Pelegri, F.J. (Ed.), Vertebrate Embryogenesis [Internet]. Humana Press, Totowa, NJ, pp. 55–75 (Methods in Molecular Biology; vol. 770). Available from: http://link.springer.com/10.1007/978-1-61779-210-6_3.
Nieuwkoop, P.D., Faber, J., 1994. Normal Table of Xenopus Laevis (Daudin), second ed. Routledge, New York, NY.
Pandur, P., Läsche, M., Eisenberg, L.M., Kühl, M., 2002. Wnt-11 activation of a non-canonical Wnt signalling pathway is required for cardiogenesis. Nature 418 (6898), 636–641, 12167861.
Papan, C., Boulat, B., Velan, S.S., Fraser, S.E., Jacobs, R.E., 2007. Formation of the dorsal marginal zone in Xenopus laevis analyzed by time-lapse microscopic magnetic resonance imaging. Dev. Biol. 305 (1), 161–171, 17368611.
Pfister, K., Shook, D.R., Chang, C., Keller, R., Skoglund, P., 2016. Molecular model for force production and transmission during vertebrate gastrulation. Development 143 (4), 715–727, 26884399.
Piekny, A.J., Glotzer, M., 2008. Anillin is a Scaffold protein that links RhoA, actin, and myosin during cytokinesis. Curr. Biol. 18 (1), 30–36, 18158243.
Piekny, A.J., Maddox, A.S., 2010. The myriad roles of Anillin during cytokinesis. Semin. Cell Dev. Biol. 21 (9), 881–891, 20732437.
Popov, I.K., Ray, H.J., Skoglund, P., Keller, R., Chang, C., 2018. The RhoGEF protein Plekhg5 regulates apical constriction of bottle cells during gastrulation. Development, 168922, 30446627.
Postlethwait, J.H., Navajas Acedo, J., Piotrowski, T., 2019. Evolutionary origin and nomenclature of vertebrate *Wnt11* -family genes. Zebrafish 16 (5), 469–476, 31295059.
Reyes, C.C., Jin, M., Breznau, E.B., Espino, R., Delgado-Gonzalo, R., Goryachev, A.B., Miller, A.L., 2014. Anillin regulates cell-cell junction integrity by organizing junctional accumulation of Rho-GTP and actomyosin. Curr. Biol. 24 (11), 1263–1270, 24835458.
Sato, N., Yonemura, S., Obinata, T., Tsukita, S., Tsukita, S., 1991. Radixin, a barbed end-capping actin-modulating protein, is concentrated at the cleavage furrow during cytokinesis. J. Cell Biol. 113 (2), 321–330, 1707055.
Sato, N., Funayama, N., Nagafuchi, A., Yonemura, S., Tsukita, S., Tsukita, S., 1992. A gene family consisting of ezrin, radixin and moesin. Its specific localization at actin filament/plasma membrane association sites. J. Cell Sci. 103, 131–143, 1429901.
Sato, A., Khadka, D.K., Liu, W., Bharti, R., Runnels, L.W., Dawid, I.B., Habas, R., 2006. Profilin is an effector for Daam1 in non-canonical Wnt signaling and is required for vertebrate gastrulation. Development 133 (21), 4219–4231, 17021034.
Serra, M., Nájera, G.S., Chuai, M., Spandan, V., Weijer, C.J., Mahadaven, L.. A mechanochemical model recapitualates distinct vertebrate gastrulation modes [Internet]. [cited 2021 Dec 30]. Available from: https://www.biorxiv.org/content/10.1101/2021.10.03.462928v2.full.pdf+html.
Session, A.M., Uno, Y., Kwon, T., Chapman, J.A., Toyoda, A., Takahashi, S., Fukui, A., Hikosaka, A., Suzuki, A., Kondo, M., van Heeringen, S.J., Quigley, I., Heinz, S., Ogino, H., Ochi, H., Hellsten, U., Lyons, J.B., Simakov, O., Putnam, N., Stites, J., Kuroki, Y., Tanaka, T., Michiue, T., Watanabe, M., Bogdanovic, O., Lister, R., Georgiou, G., Paranjpe, S.S., van Kruijsbergen, I., Shu, S., Carlson, J., Kinoshita, T., Ohta, Y., Mawaribuchi, S., Jenkins, J., Grimwood, J., Schmutz, J., Mitros, T., Mozaffari, S.V., Suzuki, Y., Haramoto, Y., Yamamoto, T.S., Takagi, C., Heald, R., Miller, K., Haudenschild, C., Kitzman, J., Nakayama, T., Izutsu, Y., Robert, J., Fortriede, J., Burns, K., Lotay, V., Karimi, K., Yasuoka, Y., Dichmann, D.S., Flajnik, M.F., Houston, D.W., Shendure, J., DuPasquier, L., Vize, P.D., Zorn, A.M., Ito, M., Marcotte, E.M., Wallingford, J.B., Ito, Y., Asashima, M., Ueno, N., Matsuda, Y., Veenstra, G.J.C., Fujiyama, A., Harland, R.M., Taira, M., Rokhsar, D.S., 2016. Genome evolution in the allotetraploid frog Xenopus laevis. Nature 538 (7625), 336–343, 27762356.
Shook, D.R., Kasprowicz, E.M., Davidson, L.A., Keller, R., 2018. Large, long range tensile forces drive convergence during Xenopus blastopore closure and body axis elongation. Elife 7, e26944, 29533180.
Shook, D.R., Wen, J.W., Rolo, A., O'Hanlon, M., Francica, B., Dobbins, D., Skoglund, P., DeSimone, D.W., Winklbauer, R., Keller, R.E., 2022. Characterization of convergent thickening, a major convergence force producing morphogenic movement in amphibians. Elife 11, e57642, 35404236.
Sive, H.L., Grainger, R.M., Harland, R.M., 2000. Early development of Xenopus laevis: a laboratory manual. In: Cold Spring Harbor. Cold Spring Harbor Laboratory Press, NY.
Sokol, S.Y., 1996. Analysis of Dishevelled signalling pathways during Xenopus development. Curr. Biol. 6 (11), 1456–1467, 8939601.
Straight, A.F., Field, C.M., Mitchison, T.J., 2005. Anillin binds nonmuscle myosin II and regulates the contractile ring. Mol. Biol. Cell 16, 9, 15496454.
Sumanas, S., Ekker, S.C., 2001. Xenopus frizzled-7 morphant displays defects in dorsoventral patterning and convergent extension movements during gastrulation. Genesis 30 (3), 119–122, 11477687.
Tada, M., Smith, J.C., 2000. Xwnt11 is a target of Xenopus Brachyury: regulation of gastrulation movements via Dishevelled, but not through the canonical Wnt pathway. Development 127 (10), 2227–2238, 10769246.
Tao, Q., Yokota, C., Puck, H., Kofron, M., Birsoy, B., Yan, D., Asashima, M., Wylie, C.C., Lin, X., Heasman, J., 2005. Maternal Wnt11 activates the canonical Wnt signaling pathway required for Axis formation in Xenopus embryos. Cell 120 (6), 857–871, 15797385.
Van Itallie, E., Kalocsay, M., Wühr, M., Peshkin, L., Kirschner, M.W.. Transitions in the proteome and phospho-proteome during early embryonic development in Xenopus [Internet]. [cited 2021 Dec 7]. Available from: https://www.biorxiv.org/content/10.1101/2021.08.05.455309v1.abstract.
Walentek, P., Schneider, I., Schweickert, A., Blum, M., 2013. Wnt11b is involved in Cilia-mediated symmetry breakage during Xenopus left-right development. PLoS One 8 (9), e73646, 24058481.
Wallingford, J.B., 2012. Planar cell polarity and the developmental control of cell behavior in vertebrate embryos. Annu. Rev. Cell Dev. Biol. 28 (1), 627–653, 22905955.
Wallingford, J.B., Harland, R.M., 2001. *Xenopus* Dishevelled signaling regulates both neural and mesodermal convergent extension: parallel forces elongating the body axis. Development 128 (13), 2581–2592, 11493574.
Wallingford, J.B., Rowning, B.A., Vogeli, K.M., Rothbächer, U., Fraser, S.E., Harland, R.M., 2000. Dishevelled controls cell polarity during Xenopus gastrulation. Nature 405 (6782), 81–85, 10811222.
Watanabe, S., Okawa, K., Miki, T., Sakamoto, S., Morinaga, T., Segawa, K., Arakawa, T., Kinoshita, M., Ishizaki, T., Narumiya, S., 2010. Rho and anillin-dependent control of mDia2 localization and function in cytokinesis. Sep 15. In: Chang, F. (Ed.), MBoC 21 (18), 3193–3204.
Wen, J.W., Winklbauer, R., 2017. Ingression-type cell migration drives vegetal endoderm internalisation in the Xenopus gastrula. Elife 6, e27190, 28826499.
Wilson, P., Keller, R.E., 1991. Cell rearrangement during gastrulation of Xenopus: direct observation of cultured explains. Development 112, 289–300, 1769334.
Winklbauer, R., 2020. Mesoderm and endoderm internalization in the Xenopus gastrula. In: Current Topics in Developmental Biology. Elsevier [Internet]. https://linkingh

ub.elsevier.com/retrieve/pii/S0070215319300754 [cited 2020 Jun 5]. p. 243–70. Available from:
Winklbauer, R., Schürfeld, M., 1999. Vegetal rotation, a new gastrulation movement involved in the internalization of the mesoderm and endoderm in Xenopus. Development 126 (16), 3703–3713, 10409515.
Yamaguchi, T.P., Bradley, A., McMahon, A., Jones, S., 1999. A Wnt5a pathway underlies outgrowth of multiple structures in the vetebrate embryo. Development 126 (6), 1211–1223, 10021340.